Computer Fraud and Security
ISSN (online): 1873-7056

Simulation Analysis of a Flexible Sports Simulation Model for Multimedia Data Analysis

Fan Huiguo, Li Xiang, Chen Dongnan*
Guilin University Of Electronic Technology, Beihai, 536000, Guangxi, China
**Email: ChenDongnan20240306@outlook.com*

Abstract:

In order to improve the analysis effect of sports simulation model, this paper proposes a flexible sports simulation model for multimedia data analysis. Moreover, the rigid body sports simulation model of the athlete is established in this paper to analyze and solve the control force required by the athlete to obtain the maximum movement distance. Besides, this paper simplifies the athlete's movement process into two stages through two constant control forces. Finally, through the force analysis of each stage, the corresponding dynamic equations are listed, and the force analysis is carried out for 7 rigid bodies separately, and the plane motion differential equations of each rigid body are listed. The experimental study shows that the simulation analysis model of a flexible sports simulation model for multimedia data analysis proposed in this paper has a good effect.

Keywords: multimedia data; flexibility; sports; model; simulation

1 INTRODUCTION

Computer simulation and analysis of human motion is a hot issue in the field of computer simulation, and it has important application value in the field of sports analysis. At present, many research institutions at home and abroad are carrying out related research work and are committed to developing simulation systems for some sports such as track and field, boxing, skiing, and table tennis. The use of these systems can greatly facilitate the training of athletes. For example, virtual athletes can accurately simulate various standard movements, and athletes can observe the execution details of the simulated standard movements from various angles during the training process. When using such a system, it is often necessary to compare the difference between the movement performed by the actual athlete and the corresponding simulated standard movement in order to analyze and evaluate the effect performed by the athlete. Video is the main storage form of athlete's motion data, which requires comparison between training video and 3D simulation results. Since the display of the action in the video is two-dimensional, the motion of the three-dimensional virtual athlete in the simulation system can be viewed from different positions and directions.

"Technology can change lives". VR is a modern computer virtual reality technology, which is of great help for the creation of virtual computer system environment. Moreover, the experiencer can also feel the virtual experience that breaks through the limitations of time and space, and the realistic effect is very strong. Whether it is action, sound or force, it is the same as the real world [1]. The application of VR technology can not only reproduce the real world, but also allow the real world to interact with the world imagined by people, and improve the fidelity of the virtual environment [2]. The actual goal of simulating VR is to process sensor data with the aid of a column sensor integration device. Based on the fusion of information, the VR virtual environment is constructed, and finally the interaction between the real world and the virtual space is realized, and its maximum value is exerted [3].

This paper applies virtual simulation technology to sports simulation, and combines multimedia data to conduct sports simulation research to improve the effect of intelligent analysis of sports.

2 RELATED WORK

Real-time simulation technology, also known as simulated real-time technology, is a technology that uses one system to imitate another real system. With the help of computer-generated virtual environment virtual simulation technology, the design scheme can be modified in real time through scheme comparison and selection. The real-time simulation virtual platform is different from the traditional 2.5-dimensional computer renderings. It integrates the environmental design and builds a virtual space concept that simulates reality for the

digitization without images, so that many complex and changeable information can be transformed into digital models [4] . It can display 360 degrees without dead ends, and comprehensively display various buildings, roads and garden plans, which not only provides new means for environmental design, but also brings new new ideas and changes in creative methods. Therefore, environmental design has become an indispensable and important part of digital construction to assist smart city planning, smart communities, smart hospitals, smart transportation, and smart sports centers [5]. And how to make the traditional environmental design more perfect from the scale, proportion, color, texture, shape and style into the construction of the future environmental design simulation virtual platform, more scientifically and reasonably predict the entire project cost, and make the overall planning effect of large-scale engineering projects. Predict and predict the cost budget in advance, reduce costs, improve efficiency for project production, and solve safety and fire hazards, and present a three-dimensional visual three-dimensional engineering project plan for project decision makers and various docking design managers and construction departments. The three-dimensional model of the simulation virtual platform reflects various environmental design schemes in an all-round way, so as to perfectly solve this series of problems [6].

Sports simulation system is an interdisciplinary subject of comprehensive sociology, management, sports training, computer science, graphics, forecasting, decision-making, psychology, mathematics, etc. The comprehensive integration of experimental science [7]. It uses the method of system analysis. Analyze the problems in the field of sports, comprehensively use mathematics, graph theory, gray theory, operations research, cybernetics, information theory and other related knowledge to build simulation models, and then use computer technology to combine graphics, spyglass, and psychology on the computer. Real-time, super-real-time, sub-real-time simulation demonstration, and finally evaluated, planned, and decided by domain experts[8]. It reproduces the coach's training experience, intention, manager's organizational plan and athletes' training process through computer simulation technology, so as to achieve the interpretation, analysis, prediction, organization and evaluation of the sports system, so as to solve the synthesis of many problems in sports training. The integration method is a strategic technology to promote the progress of sports science and technology [9]. Sports training requires the participation of athletes' multiple senses (vision, hearing, touch and smell, etc.), and the simulation of virtual reality technology emphasizes multiple perception capabilities, interactivity and immersion [10]. Therefore, with the further development of virtual reality technology, the simulation training of virtual reality technology in the field of sports will be widely used [11].

VR has been widely used in many fields such as military simulation, fire simulation, medical treatment, etc. Its purpose is to conduct simulation training for trainees in a specific environment (hostage negotiation, parachuting and fire fighting, etc.). This kind of training allows mistakes and will not The practitioner poses any risk of injury [12]. Compared with other training methods, VR-based sports simulation training has multiple perception capabilities, so it can enhance the ability of athletes to interact with the sports simulation system and improve the effect of sports training [13]. At present, there are few researches on the application of virtual environment in competitive sports training, mainly because competitive sports training has higher requirements on various performance indicators of VR system than virtual games, such as user-friendly interactivity, real-time, high precision And strong immersion, etc., coupled with the limitations of virtual reality software and hardware technology (such as virtual reality dedicated interactive equipment is relatively expensive. The existing interaction methods are not convenient and flexible enough, and the real-time performance and accuracy of the system need to be improved. These constraints Factors limit the application and promotion of VR technology in the field of competitive sports simulation training [14].

Modern competitive sports are developing rapidly to high, difficult, refined and advanced, which makes sports training rely more on modern scientific and technological means! In order to maximize the potential of people, modern sports need the continuous intervention of science and technology! Comprehensively use the discipline knowledge related to sports science, and use the methods of system science (such as system simulation) to study the inherent laws of sports. Sports system simulation is an experimental technology science [15], which is a computer simulation method. Technology reproduces the teaching experience of physical education teachers, the training intention of coaches, the organizational plan of managers and the training process of athletes, so as to achieve an experimental technical science of interpretation, analysis, prediction, organization and evaluation of the sports system! In recent years The research hotspots of system simulation include object-oriented simulation

method, qualitative simulation, distributed interactive simulation, visual simulation, multimedia simulation, etc. [16]. And object-oriented simulation method, qualitative simulation, distributed interactive simulation, visual simulation and multimedia simulation method Different, VR-based simulation emphasizes multiple perception capabilities, interactivity, and immersion, while many sports training requires the joint participation of athletes' multiple senses (such as vision, hearing, touch, and smell, etc.) [17].

3 SIMULATION ALGORITHM OF SPORTS SIMULATION MODEL OF SPORTS ATHLETE

In figure 1, h is the distance between the bottom surfaces of the two mass blocks before the athlete jumps and falls, $L_0 = 4m$ is the distance between the athlete's elastic front and the ground, H is the athlete's elastic depth, H_1 is the athlete's elastic depth in the first stage, and H_M is the maximum elastic depth of the athlete. According to the test experiment on the mechanical properties of sports ground in chapter 2, in the process of the athlete landing, we assume that the force of the sports ground on the athlete's feet is an elastic load, and the stiffness coefficient of the sports ground is represented by K=5500N/m. The two stages of the athlete's elastic process are analyzed below.

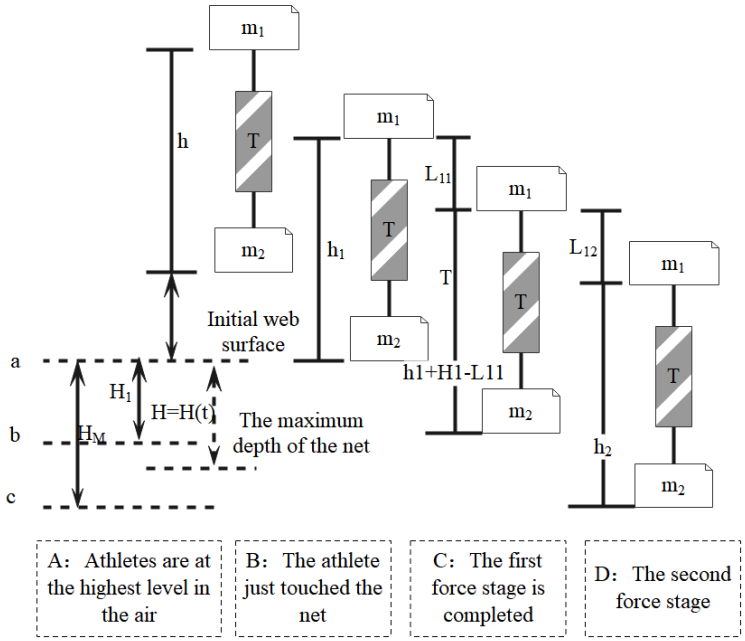

Figure 1 Schematic diagram of the two rigid body model and elastic process of sports athletes

(a) (b)

Figure 2 The force analysis diagram of the two mass blocks in the first stage

(1) The first stage of the athlete landing

The first stage of the athlete's landing is shown in figure 2.When the athlete is in the first stage of elasticity, the force analysis is carried out on the two parts of the athlete's body, where a_1 represents the acceleration of m_1, and a_2 represents the acceleration of m_2. According to the inertial parameter table of Chinese adults (GB/T17245-2004), the mass of the two rigid body parts of the athlete's body is allocated according to the

proportion of each part's mass to the total body mass, which are $m_1 = 52\,kg, m_2 = 9.5kg$, and the acceleration of gravity at the location of the experiment is $g = 9.797m/s^2$. According to figure 2, the dynamic equations of the two mass blocks in the two rigid body model can be expressed as:

$$m_1 g - T_1 = m_1 a_{11} \quad (1)$$

$$m_2 g + T_1 - KH = m_2 \ddot{H} \quad (2)$$

The initial conditions are:

$$\begin{cases} H|_{t=0} = 0 \\ \dot{H}\big|_{t=0} = v_0 \end{cases}$$

Among them, v_0 is the initial landing speed. Solving the differential formula (2), we get:

$$H = A_1\, sin(\omega t) - B_1\, cos(\omega t) + B_1 \quad (3)$$

Among them, $\omega = \sqrt{\frac{K}{m_2}}; \quad A_1 = \frac{v_0}{\omega}; \quad B_1 = \frac{m_2 g + T_1}{K}; \quad v_0 = \sqrt{2gL_0}.$

We assume that the duration of the first stage of the athlete's landing is t_1, and substituting into formula (3), we can get:

$$H_1 = A_1\, sin(\omega t_1) - B_1\, cos(\omega t_1) + B_1 \quad (4)$$

In the first stage, the height to which the mass m_1 falls is:

$$L_{11} = \frac{1}{2}\left(g - \frac{T_1}{m_1}\right) t_1^2 + v_0 t_1 \quad (5)$$

(2) The second stage of the athlete landing

T_2 represents the force between the two parts of the mass in the second stage. Similar to the analysis method in the first stage, the dynamic equations of the two mass blocks in the second stage can be expressed as (wherein, a_{12} is the acceleration of mass m_1 in the second stage):

$$m_1 g - T_2 = m_1 a_{12} \quad (6)$$

$$m_2 g + T_2 - KH = m_2 \ddot{H} \quad (7)$$

The initial conditions are:

$$\begin{cases} H|_{t=t_1} = H_1 \\ \dot{H}\big|_{t=t_1} = w[A_1\, cos(\omega t_1) + B_1\, sin(\omega t_1)] \end{cases}$$

Solving formula (7), we can get:

$$H = A_2\, sin[\omega(t - t_1)] + B_2\, cos[\omega(t - t_1)] + \frac{m_2 g + T_2}{K} \quad (8)$$

Among them, there are:

$$\begin{cases} A_2 = A_1\, cos(\omega t_1) + B_1\, sin(\omega t_1) \\ B_2 = H_1 - \dfrac{m_2 g + T_2}{K} \end{cases}$$

When the athlete has the deepest elasticity $(t = t_1 + t_2$, where t_2 is the duration of the second stage), equation (8) should satisfy:

$$\left.\frac{dH}{dt}\right|_{t=t_1+t_2} = 0 \quad (9)$$

Simultaneously equation (8) and equation (9) can be solved by solving:

$$t_2 = \frac{1}{\omega} tan^{-1} \frac{A_2}{B_2} \quad (10)$$

When the second stage is completed, the height at which m_1 drops is:

$$L_{12} = \left[v_0 + \left(g - \frac{T_1}{m_1}\right) t_1\right] t_2 + \frac{1}{2}\left(g - \frac{T_2}{m_1}\right) t_2^2 \quad (11)$$

The depth at which the athlete lands (that is, the height at which m_2 falls) is:

$$H_M = A_2 \, sin(\omega t_2) + B_2 \, cos(\omega t_2) + \frac{m_2 g + T_2}{K} \quad (12)$$

The distance between the bottom surfaces of the two masses m_1 and m_2 is denoted by h. When the athlete first touches the ground, $h = h_1$. When the athlete has the deepest elasticity, $h = h_2$. By observing the video of the sports athlete obtained in the experiment, it can be concluded that when the athlete just touches the ground, the distance between the mass centers of the two mass blocks m_1 and m_2 is 0.4m, that is, $h_1 = 0.4m$. When the athlete has the deepest elasticity, it is observed from the video that the athlete is trying to straighten his legs, and the distance between the mass centers of the two parts of the body no longer changes. Therefore, the moment h should satisfy:

$$\dot{h}\big|_{t=t_1+t_2} = 0 \quad (13)$$

Among them, there are:

$$\dot{h} = (A_2 \omega \, cos(\omega t_2) - B_2 \omega \, sin(\omega t_2)) - \left(\frac{m_1 g - T_2}{m_1} t_2 + v_0 + \left(g - \frac{T_1}{m_1}\right) t_1\right)$$

When the athlete reaches the deepest point on the ground $(t = t_1 + t_2)$, the distance h_2 between the two mass blocks can be expressed as:

$$h_2 = h_1 - (L_{11} + L_{12} - H_M) \quad (14)$$

Among them, $\Theta = h_2 - h_1$.

Combining formula (14), we can get:

$$\Theta = H_M - L_{11} - L_{12} \quad (15)$$

Because the observation of the shooting video shows that when the elasticity is the deepest, the athlete's legs are straight, and the body is basically kept upright. Therefore, the distance h_2 between the two mass blocks of the athlete should be equal to h_1 when the landing is the deepest, that is, there should be:

$$\Theta = 0 \quad (16)$$

Since formulas (13) and (16) should be satisfied at the same time, these two equations are highly nonlinear, and it is not easy to find their analytical solutions. Therefore, we give the following optimization objective function:

$$W = \left(\frac{\dot{h}}{v_0}\right)^2 + \left(\frac{\Theta}{h_1}\right)^2 \quad (17)$$

The objective function W in the above formula (17) can finally be expressed as a function of (t_1, T_1, T_2). According to the observation of the experimental video and the reports in the references, we take the minimum t_1 of not less than 0.05s, and the maximum not to exceed 0.25s, the maximum of T_1 not to exceed 3500N, and the maximum of T_2 not to exceed 3500N. Therefore, cyclic calculation can be carried out in the above range, and finally 27216 groups of (t_1, T_1, T_2, W) values can be obtained, and then the (t_1, T_1, T_2, W) values that satisfy the following conditions (18) are selected from the obtained results.

$$\begin{cases} W \to 0 \\ 0 < h_2/h_1 \leq 1 \end{cases} \quad (18)$$

Combining the selected values of (t_1, T_1, T_2) with equation (10), the time t_2 spent by the athlete in the second stage can be calculated, and combined with equation (12), the maximum depth H_M of the landing of athlete can

be calculated.

In this paper, the elastic stage of the vertical take-off process of the sports athlete is simulated and analyzed by establishing the rigid body model of the sports athlete. From the perspective of sports biomechanics, the mechanical principles and internal laws of the vertical elastic process of sports athletes are revealed. The differential equation of motion established in this paper can be used to calculate the force of each rigid body at different times. Through this model, the pushing and stretching force of sports players on the sports ground can be obtained. The modeling method can also provide a new research idea for studying other forms of sports laws.

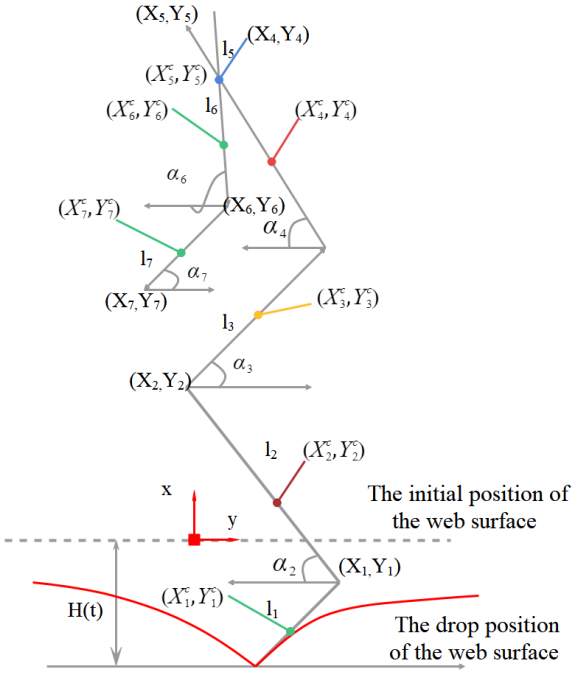

Figure 3 Schematic diagram of seven rigid body models of sports athletes

A sports athlete keeps his hand and forearm in line during vertical stretch. Therefore, the size of the hand can be ignored and the weight of the hand can be included in the forearm. We modeled the foot, calf, thigh, torso, head, upper arm and forearm (containing the weight of the hand) of the sports player as seven rigid bodies, which were labeled as rigid bodies 1, 2, 3, 4, 5, 6 and 7 in turn to build the corresponding seven-rigid body model (figure 3).

As shown in figure 3, the origin of the coordinate system is set as the fixed point in space where the contact point is when the athlete just touches the ground of the bed. We assume that the athlete only moves in the Oxy plane (it can be seen from the video that the movement bases of the left and right limbs are the same, and the movement the athlete does at this time is a plane movement). In the figure, α_i represents the angle between the i -th rigid body and the horizontal line, (x_i^c, y_i^c) represents the center of mass coordinates of the i -th rigid body, (x_i, y_i) represents the coordinates of the corresponding rigid body endpoints in the figure, and l_i represents the length of the i -th rigid body (unit: m).

Considering that the stress situation of the number 7 rigid body is the simplest, we start with the number 7 rigid body in the force analysis, and its force analysis situation is shown in figure 4. In the figure, X_6、Y_6、M_6 are the force along the x-axis direction, the force and moment in the y-axis direction, and m_7 (Table 1) is the mass of the number 7 rigid body (unit: kg). The corresponding differential equation of plane motion for the number 7 rigid body is established as shown in formula (19), where the acceleration of gravity is taken as $g = 9.797\ m/s^2$.

$$\begin{cases} m_7\ddot{x}_7^c = X_6 \\ m_7\ddot{y}_7^c = Y_6 - m_7 g \\ J_7\ddot{\alpha}_7 = M_6 + Y_6(x_6 - x_7^c) - X_6(y_6 - y_7^c) \end{cases} \tag{19}$$

The moment of inertia of the number 7 rigid body is:

$$J_7 = \frac{1}{12} m_7 l_7^2 \quad (20)$$

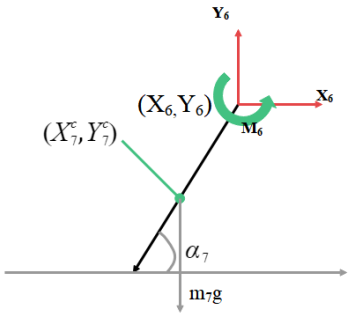

Figure 4 Force analysis diagram of No. 7 rigid body

By deforming the differential equation along the y-axis in equation (19), we can get:

$$Y_6 = m_7 \ddot{y}_7^c + m_7 g \quad (21)$$

The relationship between the center of mass acceleration and time of each rigid body can be obtained, in which the center of mass acceleration-time relationship of the forearm, the corresponding acceleration-time relationship fitting formula is equation (22), as shown below:

$$\ddot{y}_7^c = 7.6 - 654.3t + 18817.6t^2 - 93106.8t^3 + 128139.8t^4 \quad (22)$$

Substituting equation (22) into equation (21), we get:

$$Y_6 = 2.973 \times 10^5 t^4 - 2.16 \times 10^5 t^3 + 4.37 \times 10^4 t^2 - 1518t + 40.36 \quad (23)$$

Among them, t represents time, the unit is s, and the unit of acceleration is m/s^2.

The force analysis of No. 6 rigid body is shown in figure 5. In the figure, X_5、Y_5、M_5 are the force along the x-axis direction, the force and moment in the y-axis direction of the corresponding point in the figure, and m_6 is the mass of the No. 6 rigid body (unit: kg). The corresponding differential equation of plane motion for the No. 6 rigid body is established as shown in formula (24).

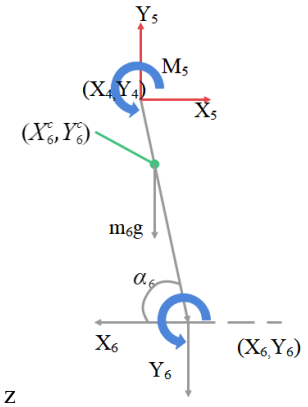

Figure 5 Force analysis diagram of No. 6 rigid body

$$\begin{cases} m_6 \ddot{x}_6^c = X_5 - X_6 \\ m_6 \ddot{y}_6^c = Y_5 - Y_6 - m_6 g \\ J_6 \ddot{\alpha}_6 = M_6 - M_5 + X_6(y_6^c - y_6) + X_5(y_4 - y_6^c) + Y(x_6 - x_6^c) \end{cases} \quad (24)$$

The moment of inertia of rigid body No. 6 is:

$$J_6 = \frac{1}{2} m_6 l_6^2 \quad (25)$$

The fitting formula of the acceleration-time relationship of the center of mass of the rigid body No. 6 is equation (26):

$$\ddot{y}_6^c = 4.5 - 524.6t + 17496.6t^2 - 89606.9t^3 + 125493t^4 \quad (26)$$

Substituting equations (26) and (23) into the second equation in equation (24), we can get:

$$Y_5 = 6.713 \times 10^5 t^4 - 4.83 \times 10^5 t^3 + 9.58 \times 10^4 t^2 - 3081t + 82.97 \quad (27)$$

By observing the video of the athlete in the process of kicking and stretching, it is found that there is no relative rotation between the athlete's head and the torso during the vertical contact with the ground during the stage of falling and kicking. Therefore, the two parts can be combined for force analysis, as shown in figure 6. In the figure, X_4、Y_4、M_4 are the force along the x-axis direction, the force and moment in the y-axis direction of the corresponding points in the figure, m_4、m_5 are the masses of the 4th and 5th rigid bodies (unit: kg), and $(x_4{}^{c'}, y_4{}^{c'})$ in the figure is the total center of mass coordinates of the rigid bodies of No. 4 and No. 5 rigid bodies combined.

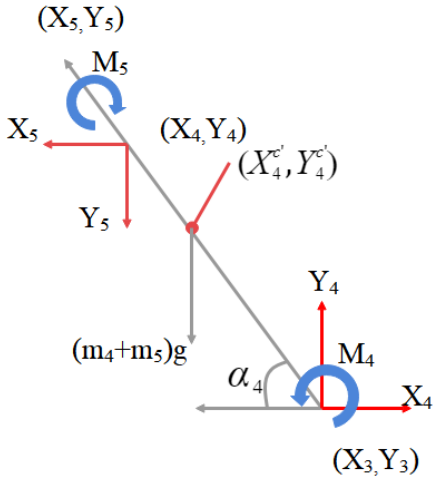

Figure 6 Force analysis diagram of rigid bodies No. 4 and No. 5

The corresponding differential equations of plane motion are established for the rigid bodies No. 4 and No. 5 as follows:

$$\begin{cases} (m_4 + m_5)\ddot{x}_4^{c'} = X_4 - X_5 \\ (m_4 + m_5)\ddot{y}_4^{c'} = Y_4 - Y_5 - (m_4 + m_5)g \\ J_{4+5}\ddot{\alpha}_4 = M_5 - M_4 - X_5\left(y_4 - y_4^{c'}\right) - Y_5\left(x_4^{c'} - x_4\right) \\ \qquad - X_4\left(y_4^{c'} - y_3\right) - Y_4\left(x_3 - x_4^{c'}\right) \end{cases} \quad (28)$$

The moment of inertia of the rigid body synthesized by the rigid bodies 4 and 5 is:

$$J_{4+5} = \frac{1}{12}m_4 l_4^2 + m_4\left[\left(y_4^{c'} - y_4^c\right)^2 + \left(x_4^{c'} - x_4^c\right)^2\right] + \frac{1}{12}m_5 l_5^2 + m_5\left[\left(y_5^c - y_5^{c'}\right)^2 + \left(x_5^{c'} - x_5^c\right)^2\right] \quad (29)$$

When the acceleration-time curves of the measured head and torso are located, the fitting formula of the acceleration-time relationship of the corresponding center of mass is equation (30):

$$\ddot{y}_4^c = -7 - 214.7t + 14488.9t^2 - 78947t^3 + 113135.5t^4 \quad (30)$$

Substituting equations (27) and (30) into the second equation in equation (28), we get:

$$Y_4 = 4.336 \times 10^6 t^4 - 3.04 \times 10^6 t^3 + 5.65 \times 10^5 t^2 - 10044t + 173.6 \quad (31)$$

The force analysis of the No. 3 rigid body is shown in figure 7. X_3、Y_3、M_3 in the figure are the force along the x-axis direction, the force and moment in the y-axis direction of the corresponding point in the figure in turn, and m_3 is the mass of the No. 3 rigid body (unit: kg).

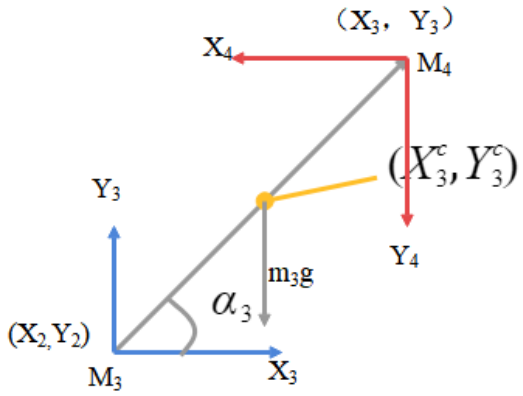

Figure 7 Force analysis of No. 3 rigid body

The corresponding kinematic differential equation for No. 3 rigid body is established as shown in formula (32):

$$\begin{cases} m_3\ddot{x}_3^c = X_3 - X_4 \\ m_3\ddot{y}_3^c = Y_3 - Y_4 - m_3 g \\ J_3\ddot{\alpha}_3 = M_3 - M_4 + X_4(y_3 - y_3^c) + X_3(y_3^c - y_2) \\ \qquad - Y_4(x_3 - x_3^c) - Y_3(x_3^c - x_2) \end{cases} \quad (32)$$

The moment of inertia of rigid body No. 3 is:

$$J_3 = \frac{1}{12} m_3 l_3^2 \quad (33)$$

The fitting formula of the acceleration-time relationship of the corresponding thigh center of mass is equation (34):

$$\ddot{y}_3^c = -8 - 136.5t + 13725.4t^2 - 75821.3t^3 + 108123t^4 \quad (34)$$

Substituting equations (31) and (34) into the second equation in equation (32), we can get:

$$Y_3 = 6.224 \times 10^6 t^4 - 4.36 \times 10^6 t^3 + 8.05 \times 10^5 t^2 - 12422t + 204.9 \quad (35)$$

The force analysis of the No. 2 rigid body is shown in figure 8. X_2、Y_2、M_2 in the figure are the force along the x-axis direction, the force and moment in the y-axis direction of the corresponding point in the figure in turn, and m_2 is the mass of the No. 2 rigid body (unit: kg).

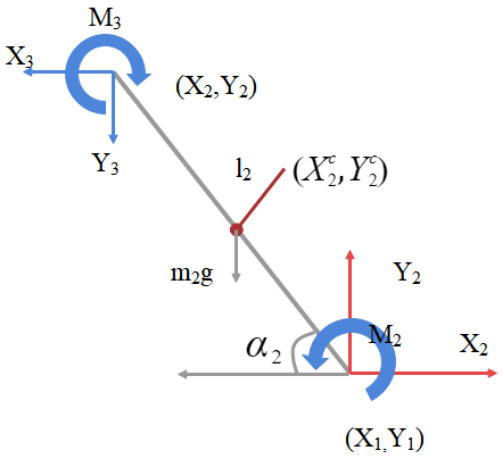

Figure 8 Force analysis of No. 2 rigid body

The corresponding differential equation of plane motion for the No. 2 rigid body is established as shown in formula (36):

$$\begin{cases} m_2\ddot{x}_2^c = X_2 - X_3 \\ m_2\ddot{y}_2^c = Y_2 - Y_3 - m_2 g \\ J_2\ddot{\alpha}_2 = M_3 - M_2 - X_3(y_2 - y_2^c) - X_2(y_2^c - y_1) \\ \qquad - X_2(y_2^c - y_1) - Y_3(x_2^c - x_2) - Y_2(x_1 - x_2^c) \end{cases} \quad (36)$$

The moment of inertia of rigid body No. 2 is:

$$J_2 = \frac{1}{12} m_2 l_2^2 \quad (37)$$

The fitting formula of the acceleration-time relationship of the corresponding calf center of mass is equation (38):

$$\ddot{y}_2^c = 2.78 - 612.6t + 19154.7t^2 - 98826.6t^3 + 140947.4t^4 \quad (38)$$

Substituting equations (35) and (38) into equation (36), we can get:

$$Y_2 = 6.861 \times 10^6 t^4 - 4.81 \times 10^6 t^3 + 8.91 \times 10^5 t^2 - 15200t + 261.8 \quad (39)$$

The force analysis of No. 1 rigid body is shown in figure 9. Y_1 in the figure is the restraint reaction force of the athlete's foot on the sports ground along the y-axis direction. Considering that the athletes studied in this chapter only perform vertical take-off, the force on the athlete's foot along the X-axis and the moment on the foot are ignored. m_1 in the figure is the mass of the foot (unit: kg).

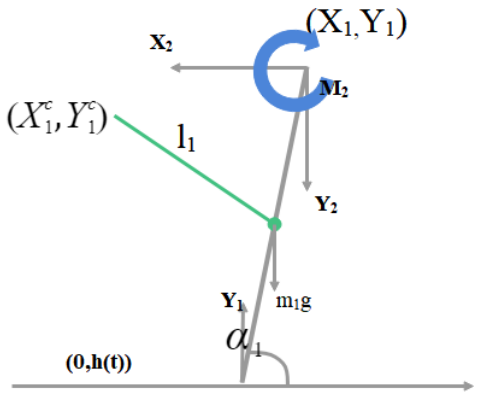

Figure 9 Force analysis diagram of No. 1 rigid body

The corresponding differential equation of plane motion for the No. 1 rigid body is established as shown in formula (40):

$$\begin{cases} m_1\ddot{x}_1^c = -X_2 \\ m_1\ddot{y}_1^c = Y_1 - Y_2 - m_1 g \\ J_1\ddot{\alpha}_1 = X_2(y_1 - y_1^c) - M_2 - Y_2(x_1 - x_1^c) - Y_1 x_1^c \end{cases} \quad (40)$$

The moment of inertia of rigid body No. 1 is:

$$J_1 = \frac{1}{12} m_1 l_1^2 \quad (41)$$

The relationship between the acceleration of the center of mass of the foot in the vertical direction and time can be obtained by curve fitting the data in the figure. The fitting formula is:

$$\ddot{y}_1^c = -8.13 - 66.2t + 12135.5t^2 - 67618t^3 + 95531.6t^4 \quad (42)$$

Substituting formulas (39) and (42) into the second equation in equation (40), we can get:

$$Y_1 = 7.034 \times 10^6 t^4 - 4.934 \times 10^6 t^3 + 9.13 \times 10^5 t^2 - 15311t + 264.8 \quad (43)$$

Formula (43) is the formula for calculating the support force of the ground on the feet of the sports athlete. The

ground force on the athlete's foot and the athlete's pushing and stretching force on the sports ground are a pair of action and reaction forces. Therefore, formula (43) is also the relationship between the vertical force (push-stretching force) F of the athlete on the sports ground and the time t.

We can also express the differential equation of motion of each rigid body uniformly as:

$$\begin{cases} m_l \ddot{x}_i^c = X_t - X_{l+1} \\ m_i \ddot{y}_i^c = Y_i - Y_{i+1} - m_i g \\ J_i \ddot{\alpha}_i = M_i - M_{i+1} - Y_{i+1}(x_i - x_i^c) - Y_i(x_i^c - x_{i-1}) \\ \qquad + X_{i+1}(y_i - y_i^c) + X_i(y_i^c - y_{i-1}) \end{cases} \quad (44)$$

Among them, m_i represents the mass of the i-th rigid body, X_i represents the force of the i-th rigid body along the x-axis at the lower endpoint as shown in figure 7, and Y_i represents the force of the i-th rigid body along the y-axis direction at the lower end point as shown in figure 7, J_i represents the moment of inertia of the i-th rigid body, and $\ddot{\alpha}_i$ represents the angular acceleration of the i-th rigid body.

4 Research on simulation effect of sports simulation model based on multimedia data analysis

Through the analysis and research of the shooting test part, the relationship between the pushing force F and the pushing time t is shown in Figure 10.

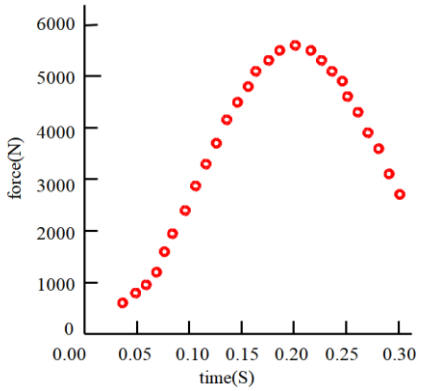

Figure 10 Relationship between pedaling force and time of seven rigid body model

By fitting the displacement (H, unit m) and time (t, unit s) curve of the athlete's foot, the corresponding fitting formula is obtained($R^2 = 0.999$):

$$H = 0.002 + 6.56t + 17.9t^2 - 217.7t^3 + 322.4t^4 \quad (45)$$

By taking the time t as a parameter, formula (43) and formula (45) are plotted together, and the relationship curve between the pedaling force (F) and the elastic depth (H) of the athlete's foot can be obtained, as shown in Figure 11.

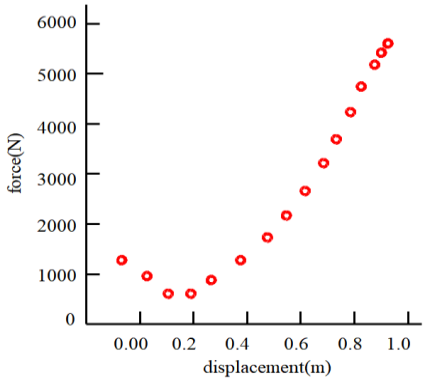

Figure 11 The relationship between the pedaling force and the elastic depth of sports athletes

From the experimental results, the relationship between the vertical force Fe on the ground and the ground descending displacement H can be obtained as (46), and the corresponding scatter diagram is shown in Figure 12.

$$F_e = 6230H^2 + 1530H \quad (46)$$

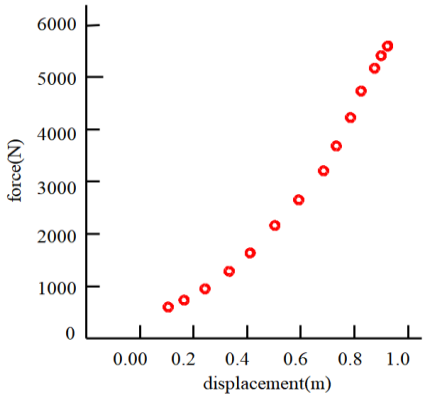

Figure 12 Load-displacement relationship diagram of sports ground

Through the above research, it is verified that the simulation effect of the sports simulation model constructed in this paper is good. On this basis, the simulation data of the model in this paper is evaluated, and the results are shown in Table 1.

Table 1 Simulation effect evaluation of sports simulation model

Number	Simulation effect	Number	Simulation effect	Number	Simulation effect
1	69.8	23	82.2	44	67.9
2	81.0	24	74.9	45	81.1
3	85.1	25	80.4	46	68.4
4	76.1	26	73.4	47	75.1
5	84.4	27	86.7	48	70.7
6	70.3	28	88.0	49	74.0
7	85.3	29	70.9	50	77.5
8	84.8	30	87.2	51	77.0
9	70.6	31	84.3	52	84.7
10	74.7	32	72.0	53	69.0
11	69.3	33	67.5	54	78.3
12	72.6	34	86.4	55	75.3
13	79.0	35	76.9	56	72.6
14	67.7	36	74.5	57	87.7
15	70.8	37	76.9	58	80.8
16	76.1	38	72.9	59	69.9
17	70.2	39	75.4	60	80.1
18	73.8	40	77.1	61	85.7
19	80.4	41	86.2	62	77.9
20	68.2	42	85.4	63	68.8
21	78.2	43	85.4	64	84.2
22	76.3				

From the above research, it can be seen that the simulation analysis model of a flexible sports simulation model for multimedia data analysis proposed in this paper has a good effect.

5 CONCLUSION

One of the key problems faced by sports simulation is how to automatically ensure that the virtual camera's viewpoint when the simulation result is displayed is the same as that of the camera when the video is captured. The existing literature shows that there is no relevant technology to solve this problem, which undoubtedly affects the application of motion simulation system in the field of sports analysis. In order to solve the above problems, a new concept of "virtual and real" contrast technology is proposed. The so-called "virtual" refers to the standard simulation actions of virtual athletes in the simulation system. This paper applies virtual simulation technology to sports simulation, and combines multimedia data to carry out sports simulation research. The research results show that the simulation analysis model of a flexible sports simulation model for multimedia data analysis proposed in this paper has a good effect.

REFERENCES

[1] Liu, S., Li, Y., & Hua, G. (2018). Human pose estimation in video via structured space learning and halfway temporal evaluation. IEEE Transactions on Circuits and Systems for Video Technology, 29(7), 2029-2038.

[2] Ershadi-Nasab, S., Noury, E., Kasaei, S., & Sanaei, E. (2018). Multiple human 3d pose estimation from multiview images. Multimedia Tools and Applications, 77(12), 15573-15601.

[3] Nie, X., Feng, J., Xing, J., Xiao, S., & Yan, S. (2018). Hierarchical contextual refinement networks for human pose estimation. IEEE Transactions on Image Processing, 28(2), 924-936.

[4] Nie, Y., Lee, J., Yoon, S., & Park, D. S. (2019). A Multi-Stage Convolution Machine with Scaling and Dilation for Human Pose Estimation. KSII Transactions on Internet and Information Systems (TIIS), 13(6), 3182-3198.

[5] Zarkeshev, A., & Csiszár, C. (2019). Rescue Method Based on V2X Communication and Human Pose Estimation. Periodica Polytechnica Civil Engineering, 63(4), 1139-1146.

[6] McNally, W., Wong, A., & McPhee, J. (2018). Action recognition using deep convolutional neural networks and compressed spatio-temporal pose encodings. Journal of Computational Vision and Imaging Systems, 4(1), 3-3.

[7] Díaz, R. G., Laamarti, F., & El Saddik, A. (2021). DTCoach: Your Digital Twin Coach on the Edge During COVID-19 and Beyond. IEEE Instrumentation & Measurement Magazine, 24(6), 22-28.

[8] Bakshi, A., Sheikh, D., Ansari, Y., Sharma, C., & Naik, H. (2021). Pose Estimate Based Yoga Instructor. International Journal of Recent Advances in Multidisciplinary Topics, 2(2), 70-73.

[9] Colyer, S. L., Evans, M., Cosker, D. P., & Salo, A. I. (2018). A review of the evolution of vision-based motion analysis and the integration of advanced computer vision methods towards developing a markerless system. Sports medicine-open, 4(1), 1-15.

[10] Sárándi, I., Linder, T., Arras, K. O., & Leibe, B. (2020). Metrabs: Metric-scale truncation-robust heatmaps for absolute 3d human pose estimation. IEEE Transactions on Biometrics, Behavior, and Identity Science, 3(1), 16-30.

[11] Azhand, A., Rabe, S., Müller, S., Sattler, I., & Heimann-Steinert, A. (2021). Algorithm based on one monocular video delivers highly valid and reliable gait parameters. Scientific Reports, 11(1), 1-10.

[12] Xu, J., & Tasaka, K. (2020). Keep your eye on the ball: Detection of kicking motions in multi-view 4K Soccer Videos. ITE Transactions on Media Technology and Applications, 8(2), 81-88.

[13] Li, Z., Bao, J., Liu, T., & Jiacheng, W. (2020). Judging the Normativity of PAF Based on TFN and NAN. Journal of Shanghai Jiaotong University (Science), 25(5), 569-577.

[14] Bhombe, J., Jethwa, A., Singh, A., & Nagarhalli, T. (2021). Review of Pose Recognition Systems. VIVA-Tech International Journal for Research and Innovation, 1(4), 1-8.

[15] Nagalakshmi Vallabhaneni, D. P. P. (2021). The Analysis of the Impact of Yoga on Healthcare and Conventional Strategies for Human Pose Recognition. Turkish Journal of Computer and Mathematics Education (TURCOMAT), 12(6), 1772-1783.

[16] Liu, J. J., Newman, J., & Lee, D. J. (2021). Using Artificial Intelligence to Provide Visual Feedback for Golf Swing Training. Electronic Imaging, 2021(6), 321-1.

[17] Martínez-González, A., Villamizar, M., Canévet, O., & Odobez, J. M. (2019). Efficient convolutional neural networks for depth-based multi-person pose estimation. IEEE Transactions on Circuits and Systems for Video Technology, 30(11), 4207-4221.